J Solid State Electrochem (2002) 6: 403–411
DOI 10.1007/s100080100243

ORIGINAL PAPER

Claude Bohnke · Jean-Louis Fourquet
Nirina Randrianantoandro · Thierry Brousse
Olivier Crosnier

Electrochemical insertion of lithium into the ramsdellite-type oxide $Li_2Ti_3O_7$: influence of the $Li_2Ti_3O_7$ particle size

Received: 12 February 2001 / Accepted: 16 July 2001 / Published online: 27 October 2001

Abstract The effect of a milling process on the electrochemical performance of $Li_2Ti_3O_7$ electrodes has been investigated by the galvanostatic intermittent titration technique (GITT) and AC impedance spectroscopy. The insertion ratio is slightly increased by the milling treatment and a value of $x_{Li} = 1.25$ per mol $Li_2Ti_3O_7$ has been determined. The average potential during insertion is close to 1.5 V/Li. The analysis of impedance data obtained at equilibrium during insertion and deinsertion shows two relaxation processes and a diffusion phenomenon at low frequency according to the Frumkin-Melik-Gayakazian model. Cycling experiments of batteries using this material were performed with unmilled and milled particles. Composite electrodes containing different amounts of electroactive material added to a binder and a conductive additive have also been prepared in order to check the effect of grinding on the cyclability of the compound. Interesting electrochemical performances have been determined with such electrodes: lithium uptake up to 1.25 Li per $Li_2Ti_3O_7$, low irreversible capacity loss between the first and the following cycles, good stability upon cycling even after 50 cycles. However, the milled process has not improved significantly the electrochemical performance of the $Li_2Ti_3O_7$ electrodes.

C. Bohnke (✉) · J.-L. Fourquet
Laboratoire des Fluorures, UMR 6010 CNRS,
Faculté des Sciences, Avenue O. Messiaen,
72085 Le Mans Cedex 9, France
E-mail: claude.bohnke@univ-lemans.fr

N. Randrianantoandro
Laboratoire de Physique de L'Etat Condensé,
UMR 6087 CNRS, Faculté des Sciences,
Avenue O. Messiaen, 72085 Le Mans Cedex 9, France

T. Brousse · O. Crosnier
Laboratoire de Génie des Matériaux,
Ecole Polytechnique de l'Université de Nantes,
Rue Christian Pauc, BP 50609,
44306 Nantes Cedex 3, France

Keywords Ramsdellite · Milling · Insertion compound · Impedance spectroscopy · Galvanostatic intermittent titration technique · Lithium-ion battery

Introduction

The insertion properties of the compounds $Li_xTi_yO_z$ with a ramsdellite structure are well known. The channels of the structure are occupied by lithium ions and contain non-occupied sites. The use of such compounds in lithium rechargeable batteries is possible either as a cathode with Li or carbon-based electrodes, but in this case the average potential of the cell is rather low (1.5 V vs. Li), or as an anode with another insertion compound like $LiMn_2O_4$ or $LiCoO_2$ [1]. In this last case, the e.m.f. of the cell should be in the range 2.3–2.7 V vs. Li. Recently, the work of Gover et al. [2] has emphasized the application of different $Li_xTi_yO_z$ compounds with the ramsdellite structure as anode materials in Li-ion batteries.

In a previous paper, the structural and electrochemical properties of $Li_2Ti_3O_7$ have been studied [3]. A maximum insertion ratio of 1.25 mol of Li for $Li_2Ti_3O_7$ has been determined, but other authors claim a maximum insertion ratio as high as two lithium per mol of $Li_2Ti_3O_7$ [4, 5]. However, conductivity measurements have demonstrated the poor electronic conductivity of $Li_2Ti_3O_7$ (about 3×10^{-9} S cm^{-1} at ambient temperature) and the necessity to mix this material with a large amount of carbon in order to initiate the insertion process. This can be a serious hindrance to the commercial use of $Li_2Ti_3O_7$ as a negative electrode in Li-ion batteries with a positive electrode commonly used like $LiCoO_2$ [6]. One way to solve this problem could be to decrease the average particle size of the active material.

In the present work, impedance spectroscopy as well as different electrochemical techniques have been used in order to determine the effect of a milling process on the performance of $Li_2Ti_3O_7$ electrodes.

Experimental

Synthesis of $Li_2Ti_3O_7$

The starting material was prepared by a solid state reaction between Li_2CO_3 and TiO_2 (anatase form) according to the reaction:

$$Li_2CO_3 + 3TiO_2 \rightarrow Li_2Ti_3O_7 + CO_2 \quad (1)$$

A single-phase compound was obtained when an excess of 7.5 mol% Li_2CO_3 was used . The starting materials (Riedel-DeHaen) from analytical grade 99% Li_2CO_3 and 99.5% TiO_2 were ground in an agate mortar. The powder was pressed into pellets under a pressure of 200 MPa. The pellets were then heated during 24 h at 750 °C in a platinum crucible to remove carbon dioxide. After a second grounding and pressing, the product was heated during 3 days at 1050 °C and quenched in air to room temperature in order to retain the ramsdellite structure, which is only stable above 940 °C.

Particle milling

$Li_2Ti_3O_7$ powder (1 g) was ball milled with a Fritsch P7 planetary milling apparatus in a zirconia jar using zirconia balls during 1 h in ethanol. The weight ratio of $Li_2Ti_3O_7$/ball was 48.5/1000. X-ray diffraction (XRD) patterns showed no structural modification between the raw material and the milled product.

Particle size measurements

The particle sizes were measured with a Coulter laser granulometer in water. The determination is based on the spherical particle model of Fraunhofer. This model gives the specific surface and the statistical size distribution of the particles. The results were obtained with the condition of a refractive index and a density of particles of 1.

Electrochemical insertion: galvanostatic intermittent titration technique and complex impedance spectroscopy

Lithium insertion has been studied by the galvanostatic intermittent titration technique (GITT) and a complex impedance technique with a Solartron 1260 FRA and an electrochemical interface Solartron 1287 connected to an AST Bravo computer. The electrochemical cell was a three-electrode set-up with two lithium foils for counter and reference electrodes. The cells were assembled in a glove box filled with argon ($H_2O = 22$ ppm; $O_2 = 0.2$ ppm). The distance between the working electrode and the reference electrode was 1 cm. The working electrode was a pellet (0.2 cm^2 area, 3 mm thickness) obtained by pressing a mixture of $Li_2Ti_3O_7$ powder, graphite powder and polytetrafluoroethylene (PTFE) in a 60%:30%:10% weight ratio. The quantity of $Li_2Ti_3O_7$ was 24 mg. A previous experiment performed with pure graphite as the working electrode had not indicated any lithium insertion within the potential window used in this study, in particular no insertion of lithium at 1 V/Li^+/Li was observed. The electrolyte was a solution of $LiPF_6$ (1 mol L^{-1}) dissolved in ethylene carbonate (EC)-dimethyl carbonate (DMC) in proportion 2:1 (Merck electrolyte Selectipur). The GITT curves during the insertion were obtained by applying a cathodic current of 40 μA during 2 h and 18 h of relaxation. After this relaxation time, the values of the potentials were constant and a quasi-equilibrium was reached. The duration of the GITT experiments were about 2 months. After 18 h of relaxation, the impedance spectrum was recorded with a 10 mV (r.m.s.) applied voltage. The typical high-frequency limit was 1 MHz and the low-frequency limit was 0.005 Hz.

Deinsertion of lithium was performed by applying an anodic current of 20 μA during 24 h and a relaxation time of 48 h. The maximum potential was fixed at 4.5 V vs. Li to prevent oxidation of the electrolyte [7].

Cycling experiments

The electrodes were prepared by mixing $Li_2Ti_3O_7$ powder with carbon black and poly(vinylidene fluoride-*co*-hexafluoropropylene) (PVDF/HFP) copolymer (Solvay) dissolved in *N*-methyl-2-pyrrolidinone (NMP). Two electrode compositions have been tested: 80% weight active material/15% weight carbon black/5% weight binder and 65% weight active material/15% weight carbon black/20% weight binder. The different compounds were mixed in a flask and the resulting mixture was homogenized during 12 h on a rotating apparatus. The paste was then coated on an aluminum current collector foil, 0.5 mm thick, using a bar-coating technique. $Li_2Ti_3O_7$-based thick films (100 μm thick) were obtained. The films were then dried over 2 h at 80 °C inside an oven. Then, 12 mm diameter disk shape samples were cut out and used as electrodes. The electrochemical tests were performed with lithium foil (Aldrich) as the negative electrode using a MacPile II potentiostat to monitor the experiments. The electrolyte was a 1 M solution of $LiPF_6$ dissolved in EC/DEC (2:1 v/v) (Merck) supported on a glass fiber filter.

During the discharge of the cell, the $Li_2Ti_3O_7$ electrode encountered lithium uptake and the charge corresponds to the removal of lithium. Cyclic voltammetric experiments were performed in the voltage range 3.5 V to 1.0 V vs. lithium with 10 mV steps every 10 s, allowing the cell to relax during 2 min at the end of each cycle. Galvanostatic initial tests were carried out by passing C/2 current through the cell in the same voltage range and with relaxation conditions as mentioned above.

Scanning electron microscopy

Observations were performed using a Leica Stereoscan 440 coupled with EDX analysis.

Results

Effect of milling on grain size

The Fraunhofer model gives the specific surface and the statistical size distribution of the particles. The values are not absolute but allow us to compare the effect of milling. The particles before milling have a mean size of 4.377 μm (in volume) with a high percentage of 13 μm diameter particles. The milled particles have a mean diameter of 0.59 μm (in volume) with two peaks at 0.3 μm and 2 μm. The ratio of the specific area after and before milling was 3.19.

The scanning electron microscopy (SEM) observations confirm the results of the granulometry experiments. The effect of milling is clearly showed in Figs. 1 and 2. The average grain size has been decreased by a factor of 10, i.e. from 10 μm for the raw material to less than 1 μm after grinding. Both powders were used for preparing electrodes by the bar-coating technique.

Open circuit potential curves

The OCV curves during insertion and deinsertion are shown in Fig. 3 in the case of the ground electroactive material. The potential variations are extremely low and permit us to conclude that a quasi-equilibrium is reached.

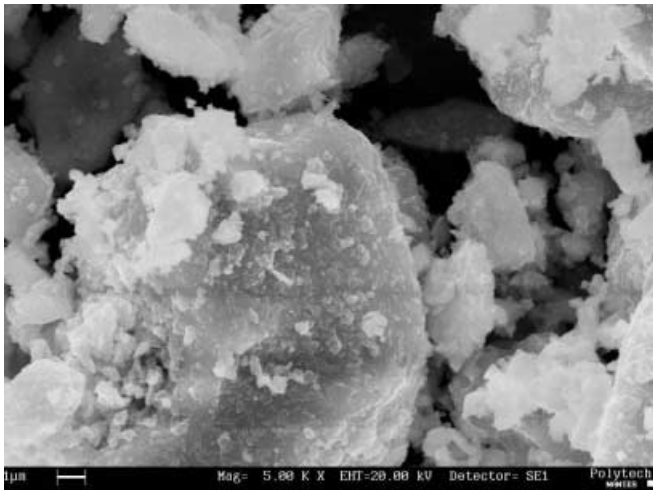

Fig. 1 SEM picture of non-milled $Li_2Ti_3O_7$ powder; the *white bar* on the left-hand side is 1 μm

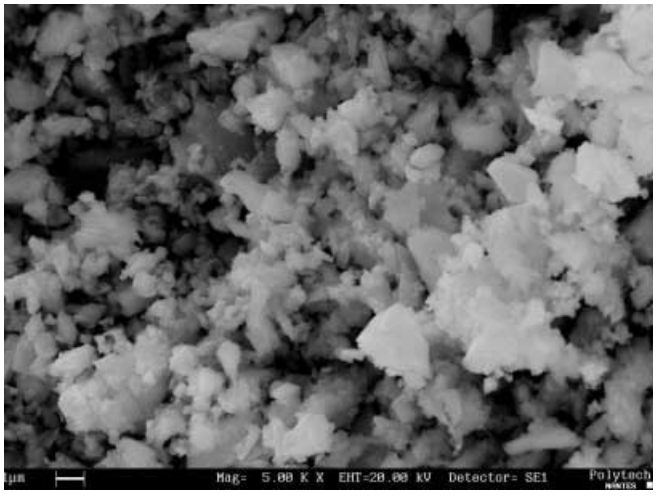

Fig. 2 SEM picture of milled $Li_2Ti_3O_7$ powder; the *white bar* on the left-hand side is 1 μm

GITT curves

The GITT insertion curves for $Li_2Ti_3O_7$ after milling are shown in Fig. 4. With the ground particles, the electrode potential varies from 1.6 V/Li to 1.2 V/Li for $x_{Li} = 0.1$–1.25. No plateau can be observed on the discharge curves, as previously obtained with unground particles in $LiClO_4$ (1 mol L^{-1}) in PC [3], but there is a regular decrease of the potential for $x_{Li} > 0.4$. The values of the potential are very close, indicating that the equilibrium is reached in both cases The maximum value of x_{Li} is slightly bigger for the ground particles (1.25 Li per mol $Li_2Ti_3O_7$ instead of 1.05 Li for unground particles).

We can observe a good reversibility of the insertion-deinsertion process, which will be illustrated by the cycling experiments. The values of E/Li are of the same order during the insertion and the deinsertion. The

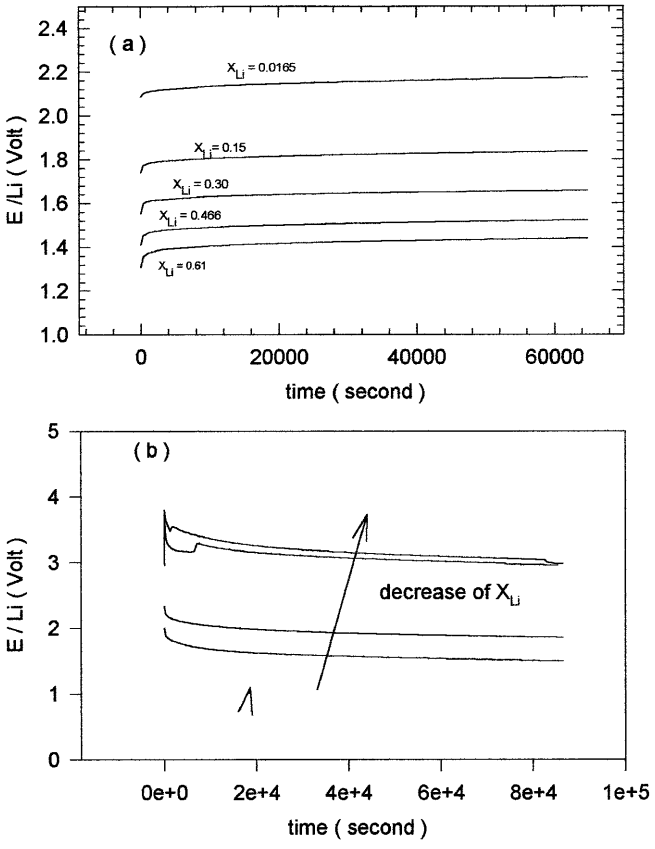

Fig. 3 **a** Open circuit voltage after galvanostatic discharges (insertion at $i = -40$ μA during 2 h). **b** Open circuit voltage after galvanostatic charges (deinsertion at $i = +20$ μA during 24 h)

capacity during the discharge is about 123 mA h g^{-1}. This value is lower than the values obtained by Gover et al. [2] and Arroyo y de Dompablo et al. [5]. In the latter paper the authors observed the formation of a new phase for $0.6 < x_{Li} < 1.9$. The experimental details indicate a fast insertion rate and it is doubtful that the GITT curve was obtained at equilibrium or quasi-equilibrium, in contrast to our work. A second phase appeared which is not $Li_{2+x}Ti_3O_7$ in any case.

Impedance measurements and an electrical model

Figure 5 shows the impedance diagrams in the Nyquist plane recorded under open-circuit conditions after complete relaxation of the electrode. The Bode plots (not shown here) indicate two relaxation processes. The first one has a maximum phase angle varying from 4 to 32 Hz with the insertion ratio, and the second one has a maximum phase angle at 500–1600 Hz. The low-frequency domain in the Nyquist plane displays a linear behavior with an angle lower than 45° versus the real axis, thus indicating a non-ideal diffusion process in the low-frequency domain below 50 mHz.

In the Nyquist plane, the circles fitted by geometrical adjustments are not centered on the real axis, indicating

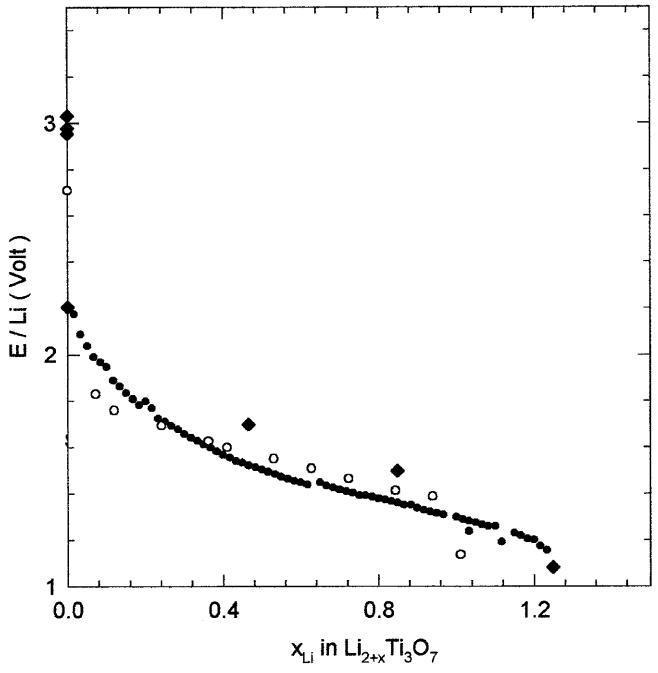

Fig. 4 Galvanostatic intermittent titration curve obtained with the composite electrodes carbon/$Li_2Ti_3O_7$/PTFE (60:30:10 in weight). *Small solid circles*: ground $Li_2Ti_3O_7$ (insertion); *open circles*: unground $Li_2Ti_3O_7$ (insertion) [3]; *large solid circles*: ground $Li_2Ti_3O_7$ during the deinsertion

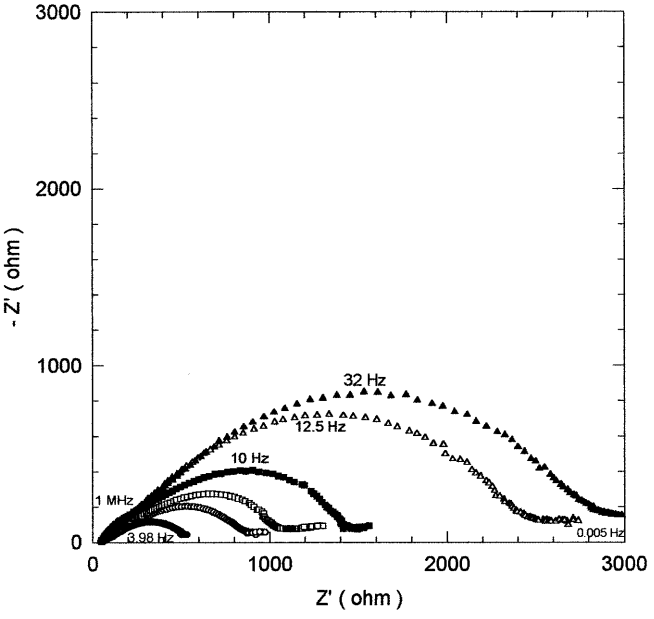

Fig. 5 Impedence plot in the Nyquist plane obtained with a composite electrode of carbon/ground $Li_2Ti_3O_7$/PTFE at different lithium insertion ratios: *solid lozenges*: $x_{Li}=0.15$; *open circles*: $x_{Li}=0.42$; *open squares*: $x_{Li}=0.70$; *solid squares*: $x_{Li}=0.81$; *open triangles*: $x_{Li}=1.04$; *solid triangles*: $x_{Li}=1.25$

one or more constant elements. We observe a similar shape when the lithium insertion ratio increases.

In order to model the electrical behavior of the electrode, an electrical model has been used and the data have been fitted with the Zview program (Scribner Solartron). This program allows us to take into account the non-ideal behavior of the electrical components (constant phase elements).

In order to take into account the different processes which take place during the electrochemical insertion, we propose to use the electrical model shown in Fig. 6. The notations are those of the Scribner fitting program (Fig. 6a). This model involves the ohmic resistance R1 made of the electrolyte and the electrode resistances. The two relaxation processes are modeled by two distributed elements, DE1 and DE2, with resistances DE1-R and DE2-R and capacitance analogs DE1-T and DE2-T associated with a constant phase angle characterized by an exponent φ. The impedance of the element can be calculated by:

$$Z = \frac{R}{1 + RT(j\omega)^{\varphi}} \tag{2}$$

The low-frequency linear part of the diagram is modeled by:

$$Zd = \frac{1}{T(j\omega)^{\varphi}}. \tag{3}$$

The diffusional impedance is given by $Z_w = W(1-j)^{1/2}\omega^{-1/2}$; hence, in the case of non-ideal behavior as obtained with our experiment:

$$W = 1/T(2)^{\varphi} \tag{4}$$

The fitting of the results using the program gives a global error and individual error on each component. The global average error on all our results is less than 5%. The fitting procedure has been applied to 75 impedance spectra during the insertion and 7 spectra during the deinsertion.

The physical model of Frumkin-Melik-Gayakazian shown in Fig. 6b gives the meaning of the DE*i* component. The high-frequency resistance is the electrolyte-electrode resistance. DE1-T and DE1-R model a multilayer surface film (transmission line). DE2-T and DE2-R are respectively the double layer capacity and the charge transfer resistance between the multilayer surface film and the electroactive grains. The Warburg impedance is linked to the diffusion of lithium in the grains. An example of the fitting results is shown in Fig. 7 in the Nyquist plane.

The fitting procedure leads to the determination of the kinetic parameters of the electrochemical process (i.e. the exchange current is proportional to the inverse of the charge transfer resistance) and the electrical components linked to the lithium insertion ratio x_{Li}.

The variations of the resistances DE*i*-R are described in Fig. 8. The capacitance analog DE*i*-T (with $i=1$ or 2) values plotted as a function of the insertion ratio x_{Li} are shown in Fig. 9. The diffusion coefficient values are calculated with the equation [9]:

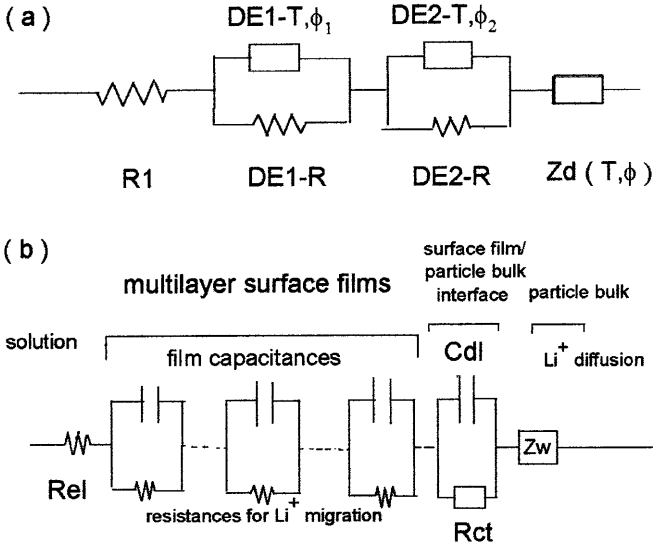

Fig. 6 **a** Equivalent electrical model for the carbon/$Li_2Ti_3O_7$/PTFE electrode using the Scribner Solartron fitting program. **b** The Frumkin- Melik-Gayakazan model [8]

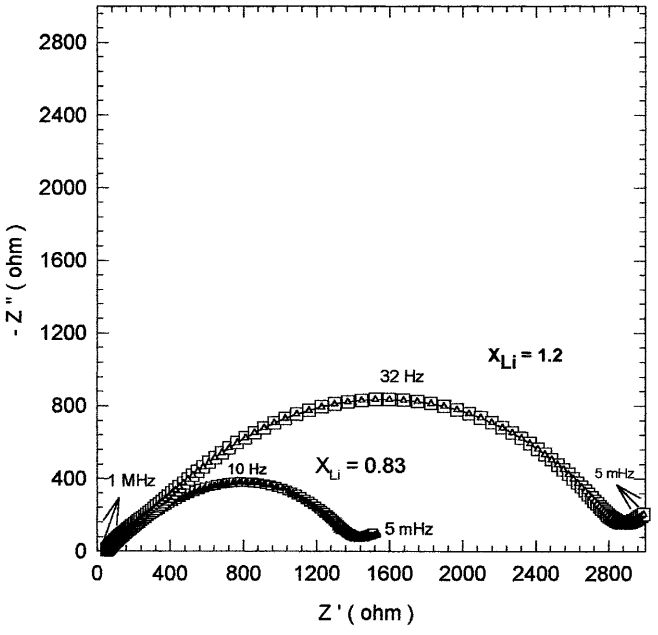

Fig. 7 Examples of fitting obtained with the Scribner program for two impedance data: *open squares*: experimental data; *open triangles*: calculated values

$$W = \frac{V\mathrm{m} \cdot \mathrm{d}E/\mathrm{d}x}{nFA\left(2\tilde{D}\right)^{1/2}} \tag{5}$$

The symbols are: W, obtained by Eq. 3; V_m, the molar volume of $Li_2Ti_3O_7 = 84.76$ cm^3 mol^{-1}; $\mathrm{d}E/\mathrm{d}x$, calculated with the $E = f(x_{Li})$ curve; $n = 1$; $F = 96493$ C; A = geometrical area of the sample (cm^2); $\tilde{D}$ = diffusion coefficient (cm^2 s^{-1}).

We suppose a diffusion of lithium ions in the inserted material and also that the surface is flat and

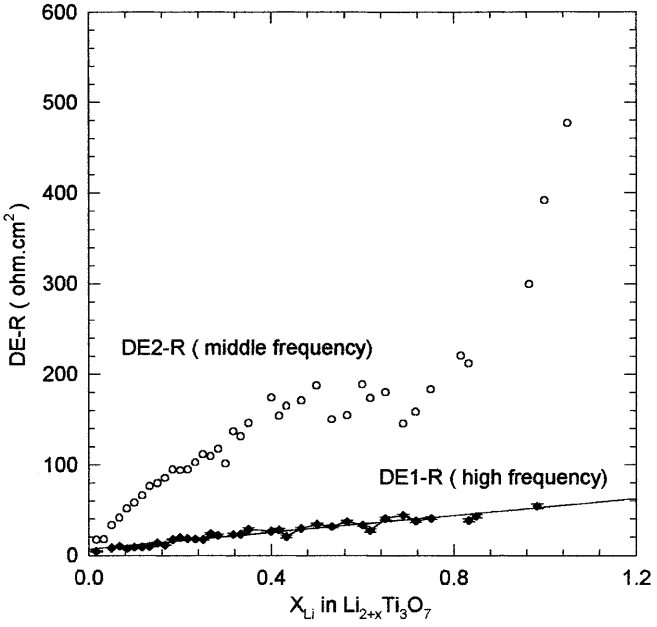

Fig. 8 Variations of the DE*i* resistances versus the lithium insertion ratio for ground $Li_2Ti_3O_7$. Errors on the fitted values are quoted for the resistance R1. *Open circles*: resistance DE2-R for the geometrical area 1 cm^2; *solid diamonds*: DE1-R for the geometrical area 1 cm^2

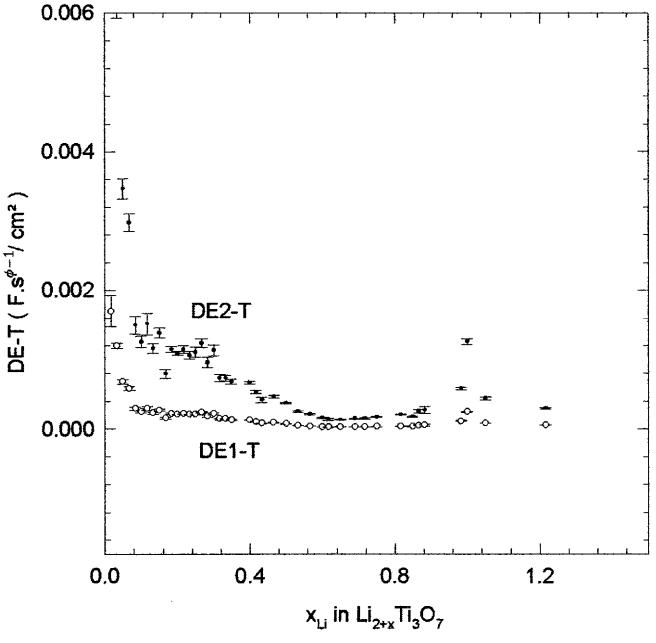

Fig. 9 Variations of the pseudo-capacitances DE*i*-T with the errors on the fitted values for ground $Li_2Ti_3O_7$. *Solid circles*: middle frequency capacitance for a geometrical electrode of area 1 cm^2; open circles: high-frequency capacitance for a geometrical electrode of area 1 cm^2

no diffusion of lithium occurs in the passive layer. The values decrease by three orders of magnitude in the first steps of insertion for the ground material (ca. 10^{-10} cm^2 s^{-1} for $x_{Li} = 1.25$), while the variations

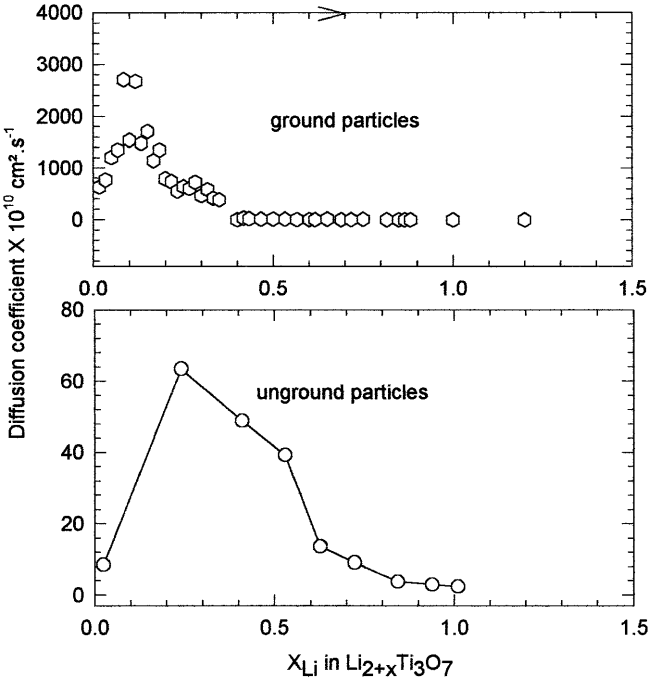

Fig. 10 Variations of the apparent diffusion coefficient of lithium for ground and unground $Li_2Ti_3O_7$ (calculated with data from [3])

for the unground material calculated with the data of the previous paper [3] are less important (Fig. 10). These results point out the limitation of the model used and indicate that the values are not the real diffusion coefficient values. A better model using the insertion in spherical particles [10] should give more realistic values.

Discussion

With unground material, the impedance diagrams were characterized by two relaxation processes instead of only one as described in a previous paper [3]. The diffusion process was observed over a wide range of frequencies (15 mHz to 4 Hz). The two relaxations are well defined for the high insertion ratios.

With ground particles, we observe two relaxations for all the x_{Li} range. The diffusion impedance is observed below 50 mHz. The high-frequency relaxation (f= 500–1500 Hz) is characterized by the φ exponent value, which increases linearly from 0.5 to 0.8 when x_{Li} varies from 0 to 0.6. The φ exponent value for the second relaxation (4–32 Hz) increases with the same variation. This indicates a decrease of the inhomogeneities in the electrical medium. Finally, the milling process increases the values of the relaxation frequencies. For the ground particles, we observe a linear increase as predicted by the empirical formula DE1-R (ohm·cm^2) = $4.7x_{Li} + 6.6$, obtained by linear regression ($r^2 = 0.99$). We suppose that the increase of the multilayer surface film thickness increases DE1-R. In the same way, the effect of milling causes the increase of the DE2-R values. However, in this latter case, the variations are linked to the insertion ratio with a singularity for $x_{Li} = 0.6$ and this indicates a different behavior of the electroactive material during the insertion process if x_{Li} is higher or lower than 0.6.

The values of DE*i*-T are of the same order of magnitude (1–10 mF $s^{\phi-1}$ cm^{-2}) with a ratio of 3 between the two pseudo-capacitances. An important decrease appears for $x_{Li} = 0.6$. Nevertheless, these values are very high in comparison with those reported for $LiCoO_2$ [7].

The presence of multilayer surface films of Li_2CO_3 may explain the high-frequency relaxation as described for $LiCoO_2$ by Levi et al. [8] and other authors [11] with $LiPF_6$ in EC:DMC and by Maurin et al. [12] with carbon nanotubes. The growth of this layer is clearly shown by the increase of the DE1-R resistance in the $LiPF_6$-EC/DMC electrolyte. The middle frequency relaxation (around 10 Hz) can be attributed to the charge transfer resistance/double layer capacitance of the electrochemical reaction:

$$Li^+ + e \rightarrow Li(host) \quad (6)$$

With regard to the capacity of insertion, as a general rule, the lithium insertion involves an electron transfer to titanium and reduces the valence of titanium from (IV) to (III). The maximum x_{Li} obtained for the $Li_2Ti_3O_7$ raw material is 1. This value is increased to 1.2 for the ground material. This is very low if a reduction of all titanium is expected in $Li_2Ti_3O_7$. In fact, this low value is linked to the number of vacancies in the structure. The value of $x_{Li} = 0.6$ corresponds rigorously to the occupation of half of the vacancies of lithium in the ramsdellite network. The structural formula $Li_{2.29}(Ti_{3.43}\square_{0.57})O_8$ chosen for $Li_2Ti_3O_7$ in the previous paper is in good agreement with the impedance data. This value of 0.6 indicates a total filling of the lithium site called C4 by Grin and West [13]. The other site (C1) is energetically less favorable to the insertion. The charge transfer resistance (DE2-R) values are linked to the energy difference between the sites. This was also observed by electrochemical spectroscopy at low scan rates [3]. Arroyo y de Dompablo et al. [4] observed, with a fast insertion rate, the formation of a new phase for $x_{Li} > 0.6$. However, for $x_{Li} > 1.25$, the unit cell lattice parameter and the unit cell volume of $Li_{2+x}Ti_3O_7$ remain constant. On the basis of our results we can say that the excess lithium is not inserted in $Li_{2+x}Ti_3O_7$.

The diffusion coefficient measurements are not within the same order of magnitude for ground and unground material, but the model used is critical and a new model taking into account the grain shape and grain size distribution should give more realistic values.

Cycling tests

Cycling experiments were performed in order to confirm that $Li_2Ti_3O_7$ can be used as an anode for Li-ion bat-

teries. First, the bar-coated electrodes were tested using cycling voltammetry in order to confirm that the electrochemical window can be the same as for the GITT experiments (3.5V to 1.0 V vs. Li^+/Li) (Fig. 11). At least, three cathodic and three anodic current peaks can be observed, indicating the complexity of the whole insertion/deinsertion processes.

The raw powder (non-milled powder) electrodes were first tested. In Fig. 12a and b are indicated the first three complete cycles for electrodes containing respectively 80% and 65% of raw $Li_2Ti_3O_7$ powder, with a cycling rate of C/2 for the first intercalation. In both cases, approximately 1.3 Li per $Li_2Ti_3O_7$ can be inserted into the host structure. Moreover, the irreversible loss occurring during the first cycle is similar and relatively low, about 0.1 Li per $Li_2Ti_3O_7$. These results are quite consistent with the GITT experiments despite the lower values of the cycling current used for the coulometric titration. Electrodes of the same composition were prepared using the milled powder (80% and 65% of milled $Li_2Ti_3O_7$ powder). Figure 13a and b also shows the first three cycles of these electrodes. The cycling rate is C/2.5. The electrochemical behavior of these electrodes is very similar to the previous ones. The intercalation rate (1.2 Li per unit cell) seems slightly decreased by the milling process, but this variation is within the error range on the weight of active material and therefore can hardly be assigned to the milling process.

However, the most visible effect of the milling process can be seen in the irreversible loss occurring during the first reduction, which is slightly increased (0.15–0.3 Li per $Li_2Ti_3O_7$) compared to the non-milled material. The irreversible capacity loss is more important when the amount of active material is high (80%). The experiment was repeated and the irreversible capacity loss is always increased with 80% weight milled powder of $Li_2Ti_3O_7$.

However, the 65% milled powder facilitates the bar-coating process and leads to a better aspect of the electrodes. Subsequently, this composition of milled powder was chosen to carry out further electrochemical tests.

Up to 50 cycles are shown in Fig. 14 for a $Li_2Ti_3O_7$ electrode (65 wt% of milled material) with a cycling rate of C/3. The first lithium insertion leads to a specific capacity of 125 mA h g^{-1} and a reversible capacity of 100 mA h g^{-1} is obtained over more than 50 cycles. One can observe the very good stability of the capacity upon cycling. The insertion/deinsertion process that occurs in the ramsdellite structure does not involve any destruction of the $Li_2Ti_3O_7$ electrode and leads to a very good cyclability. Such behavior has already been observed in titanium-based oxides investigated as possible negative electrodes in lithium ion batteries [14].

Finally, in order to determine the average cell potential of a complete cell using the titanate as the negative electrode and a commercial cathode material, a $Li_2Ti_3O_7$ electrode containing 80% of raw material was tested as an anode in a three-electrode cell versus a $LiCoO_2$ cathode (80% $LiCoO_2$/15% carbon black/5% PVDF/HFP), using a lithium ring as reference electrode. An excess of $LiCoO_2$ was used. The voltage limits for the galvanostatic experiments at a C/2 rate were set at 1.0 V and 3.5 V for the $Li_2Ti_3O_7$ negative electrode with

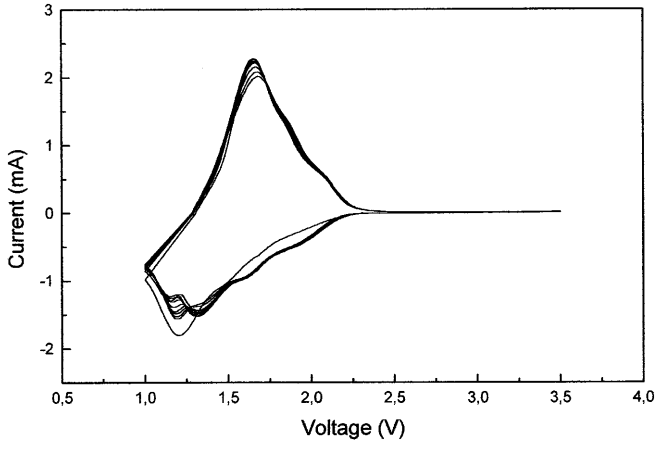

Fig. 11 Typical cyclic voltammogram of 2 mg $Li_2Ti_3O_7$ electrodes (12 mm diameter) cycled with 10 mV steps every 10 s between 3.5 V and 1.0 V vs. Li^+/Li

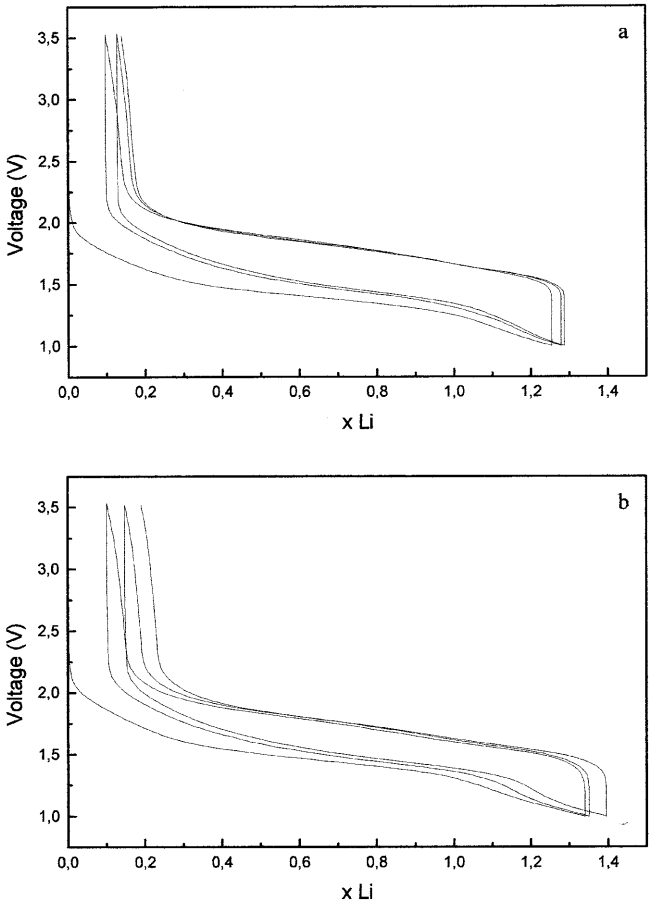

Fig. 12 First three cycles (galvanostatic mode) at C/2 rate between 1.0 V and 3.5 V vs. Li^+/Li for 2 mg electrodes containing respectively **a** 80% and **b** 65% unground $Li_2Ti_3O_7$

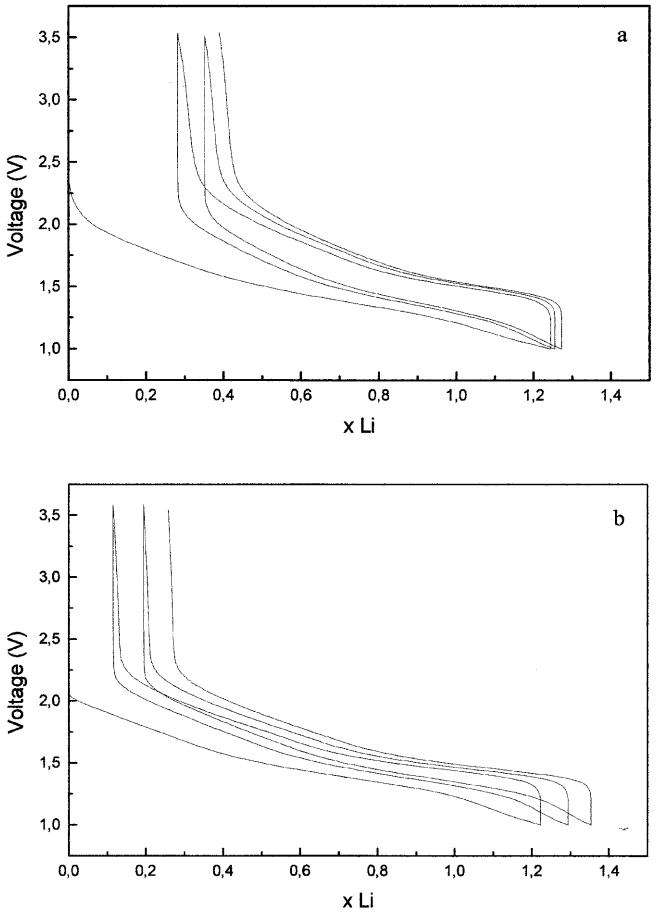

Fig. 13 First three cycles (galvanostatic mode) at C/2.5 rate between 1.0 V and 3.5 V vs. Li^+/Li for 2 mg electrodes containing respectively **a** 80% and **b** 65% unground $Li_2Ti_3O_7$

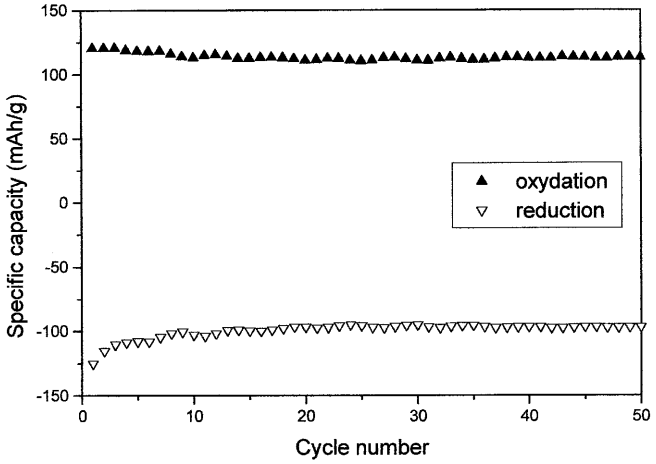

Fig. 14 Specific capacity vs. cycle number for 2 mg electrodes containing 65% of ground $Li_2Ti_3O_7$ cycled galvanostatically at C/3 rate

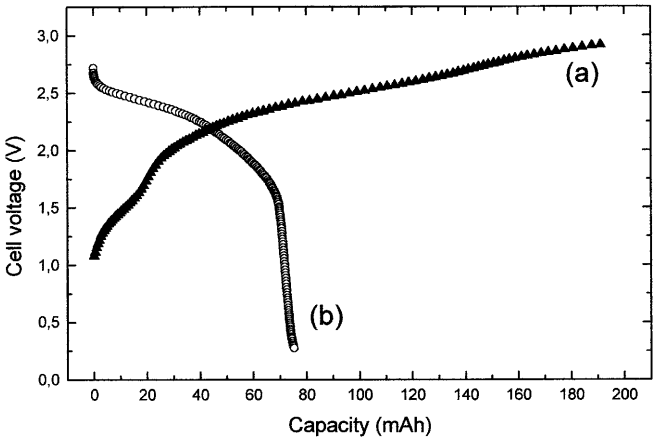

Fig. 15 Cell voltage versus cell capacity for the first two cycles of 2 mg unground $Li_2Ti_3O_7$ electrodes (85 wt% active material) cycled versus a $LiCoO_2$ cathode (C/7 rate). Curves (*a*) and (*b*) show the voltage associated with the first insertion and deinsertion, respectively

respect to the lithium reference electrode. Figure 15 shows the two first cycles of the cell thus prepared, during both insertion and deinsertion. The average cell voltage associated with this type of battery is included in the voltage range 2–2.5 V. It could be increased in further experiments by using "high potential" cathodes like Ni- or Cu-doped manganates [15, 16, 17].

Conclusion

The electrochemical performances of ground and unground $Li_2Ti_3O_7$ electrodes have been studied. The impedance diagrams during the lithium uptake show an insertion reaction not reduced to the charge transfer/diffusion sequence. The presence of a second reaction linked to the formation of a passive layer generally attributed to the Li_2CO_3 compound is observed when the electrolyte is $LiPF_6$ in EC/DMC. The reversibility of the insertion process is good despite the formation of this passive layer.

The use of the $Li_2Ti_3O_7$ ramsdellite compound in a rechargeable lithium battery seems possible. A reproducible reversible capacity of 100 mA h g^{-1} can be obtained over more than 50 cycles using a bar-coated electrode containing the electroactive material, a PVDF/HFP binder and carbon black. The average voltage versus a metallic lithium electrode is 1.2 V, which is higher than for carbon-based material and which can also provide better safety to the battery. However, the milling process experiments with the $Li_2Ti_3O_7$ powder do not significantly increase the electrochemical performances of this material. This could be due to the passivation layer, which can be partially made of Li_2CO_3 in the $LiPF_6$ EC/DEC electrolyte.

A "rocking chair" lithium cell with $LiCoO_2$ as the positive electrode has been designed. An average voltage of 2–2.5 V can be obtained from the cell. The next investigation will be a grinding of carbon and the electroactive material together, as described in a recent

communication [18]. This will permit an enhancement of the capacity of the electrode and allow a better performance for use in a lithium battery as an anode versus a high-voltage cathode like Ni- or Cu-doped manganates.

Acknowledgements We acknowledge Dr. J.P. Pereira-Ramos from Lesco, Thiais (France), for providing the $LiCoO_2$ powder.

References

1. Blyr A, Sigala C, Amatucci G, Guyomard D, Chabre Y, Tarascon JM (1998) J Electrochem Soc 145:194
2. Gover RBK, Tolchard JR, Tukamoto H, Murai T, Irvine JTS (1999) J Electrochem Soc 142:4348
3. Garnier S, Bohnke C, Bohnke O, Fourquet JL (1996) Solid State Ionics 83:323
4. Arroyo y de Dompablo ME, Moran E, Varez A, Garcia-Alvarado F (1997) MRS Bull 32:993
5. Arroyo y de Dompablo E, Varez A, Garcia-Alvarado F (2000) J Solid State Chem 153:132
6. Mizushima K, Jones PC, Wiseman PJ, Goodenough JB (1980) Mater Res Bull 15:783
7. Guyomard D, Tarascon JM (1995) J Power Sources 54:92
8. Levi MD, Salitra G, Markovski B, Teller H, Aurbach D, Eider U, Heider JL (1999) J Electrochem Soc 146:1279
9. Ho C, Raistrick ID, Huggins RA (1980) J Electrochem Soc 127:343
10. Meyer JP, Doyle M, Darling RM, Newman J (2000) J Electrochem Soc 147:2930
11. Rodrigues S, Munichandraiah N, Shukla AK (1999) J Solid State Electrochem 3:397
12. Maurin G, Bousquet C, Henn F, Almayrac R, Bernier P, Simon B (1999) Proc Colloq Groupe Fr Etude Composés Insert 83
13. Grins J, West AR (1986) J Solid State Chem 65:265
14. Colbow KM, Dahn JR, Haering RR (1989) J Power Sources 26:397
15. Zhong Q, Bonakdarpour A, Zhang M, Gato Y, Dahn JR (1997) J Electrochem Soc 144:205
16. Ein-Eli Y, Howard WF, Lu SH, Mukerjee S, McBreen J, Vaughey JT, Thackeray J (1998) J Electrochem Soc 145:1238
17. Ein-Eli Y, Vaughey JT, Thackeray MM, Mukerjee S, Yang XQ, McBreen J (1999) J Electrochem Soc146:908
18. Lenain C, Aymard, L. Courvoisier L, Salver-Disma F, Tarascon JM Actesxx (1999) Proc Colloq Groupe Fr Etude Composés Insert 12